Measurements of inclusive and differential top quark pair cross-section at the LHC

Peter Hansen, University of Copenhagen

On behalf of the ATLAS and CMS collaborations

TOP2022 Conference

Durham, September 5, 2022

Top pair cross-section measurements at the LHC

OUTLINE:
1. ATLAS+CMS Run1 combination of eμ channel x-section.
2. Inclusive x-section at 5.02 TeV
3. Differential x-sections at 13 TeV in the dilepton channel
4. Differential x-sections at 13 TeV in the lept.+jets channel
5. Differential x-sections at 13 TeV in the ”all-jets” channel

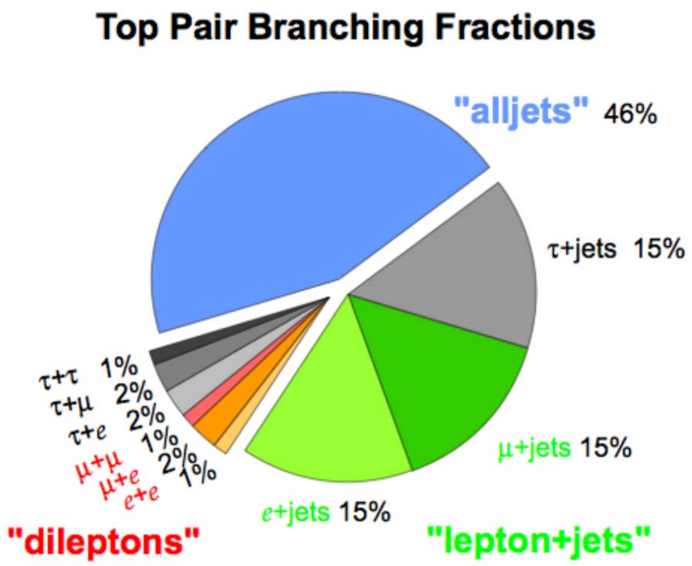

Run2 produced ~200M top pairs in ATLAS+CMS at 13 TeV!
Some leading order diagrams:

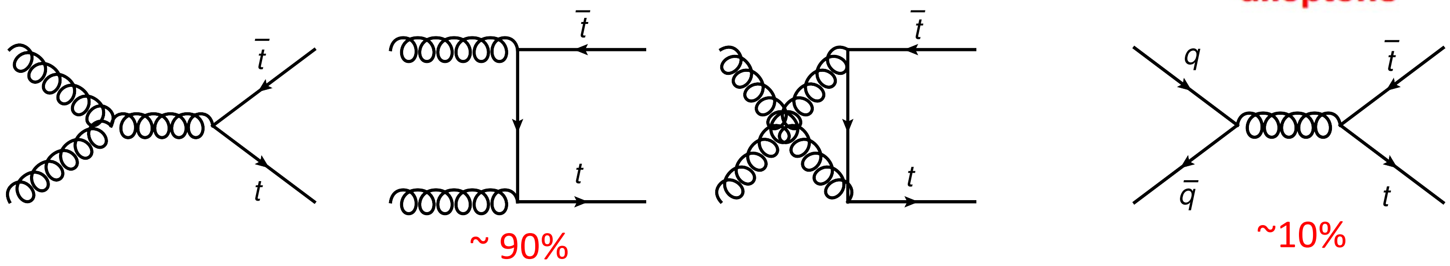

The reported measurements are compared with predictions from models. See also next talk by Rene Poncelet.
Very accurate QCD models are needed to extract important constants – such as m_t - from the data
(See Matteo Defranchis talk this afternoon).

ATLAS+CMS top pair combination at 7 and 8 TeV

- ATLAS counts events, N_1 and N_2 , with one or two b-jets in the "golden" eμ channel,
and extracts the cross-section and the b-tagging efficiency from the two equations:

$$N_1 = L\sigma_{t\bar{t}}\, \epsilon_{e\mu} 2\epsilon_b(1 - C_b\epsilon_b) + N_1^{\mathrm{bkg}}$$
$$N_2 = L\sigma_{t\bar{t}}\, \epsilon_{e\mu} C_b {\epsilon_b}^2 + N_2^{\mathrm{bkg}}$$

- CMS uses a global profile likelihood fit to all eμ events with input also from additional jets
- The two measurements are then combined using the Convino tool

This yields a ~25% reduction of uncertainties and legacy inclusive cross-sections:

$$\sigma_{t\bar{t}}\ (\sqrt{s} = 7\ \mathrm{TeV}\ ) \quad = \quad 178.5 \pm 4.7\ \mathrm{pb}$$
$$\sigma_{t\bar{t}}\ (\sqrt{s} = 8\ \mathrm{TeV}\ ) \quad = \quad 243.3^{+6.0}_{-5.9}\ \mathrm{pb},$$

The results are used for an accurate determination of

$$\alpha_S(m_Z) = 0.1170^{+0.0021}_{-0.0018}$$

as well as a new determination of m_t^{pole} (see Matteo's talk)

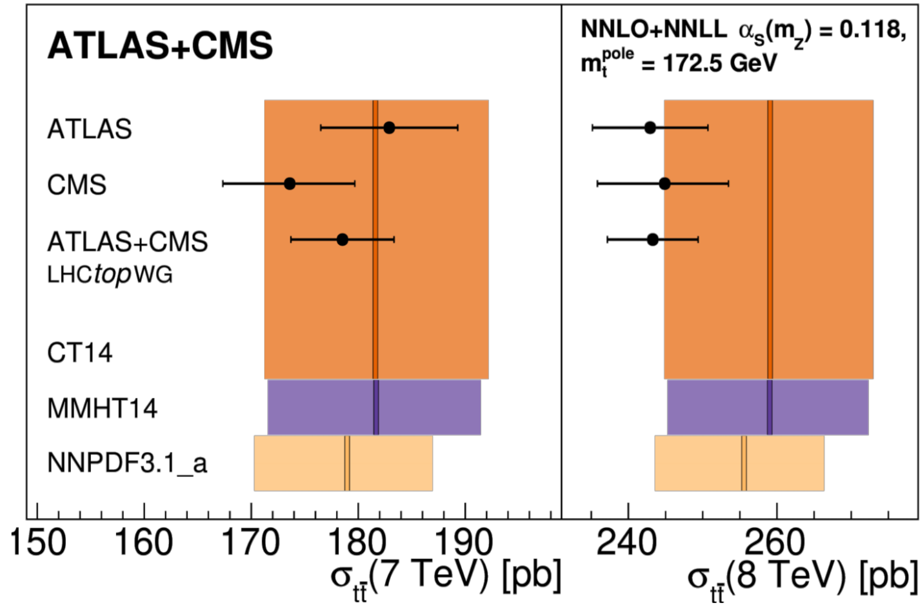

arXiv:2205.13830

Top pair inclusive cross-section at 5.02 TeV

arXiv:2207.01354

JHEP04 (2022) 144

- ATLAS + CMS recorded 257pb^{-1} + 302pb^{-1} at 5.02 TeV in 2017 and measured the top pair x-section. This is much smaller than at higher collision energies because of the steeply falling gluon PDF. Furthermore, the $q\bar{q}$ fraction is twice that at 13 TeV, and *x* is higher, offering new PDF constraints.

- In the ATLAS analysis, all dilepton channels were included and combined with the l+jets channel using the Convino tool . The combined result has an uncertainty of 3.9% .

- The CMS analysis combines a new measurement using the eμ channel in 2017 data with a measurement using l+jets in 27pb^{-1} of 2015 data (the combination uses an iterative BLUE method)

ATLAS: $\sigma_{tt} = 67.5\ \pm 0.9(stat)\ \pm 2.3(syst) \pm 1.1(lumi) \pm 0.2(beam)$ pb
CMS : $\sigma_{tt} = 63.0\ \pm 4.1(stat)\ \pm 3.0(syst + lumi)$ pb

NNLO QCD: $(\text{Top++}, m_t = 172.5\ GeV)$

$\sigma_{t\bar{t},pred} = 68.2^{+5.2}_{-5.3}$ pb

The results agree with each other and with the QCD prediction

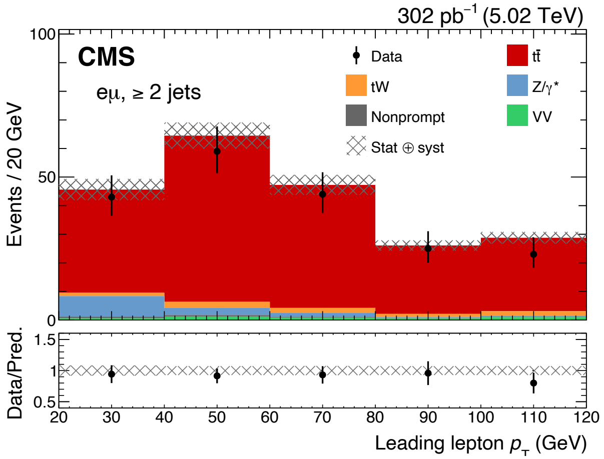

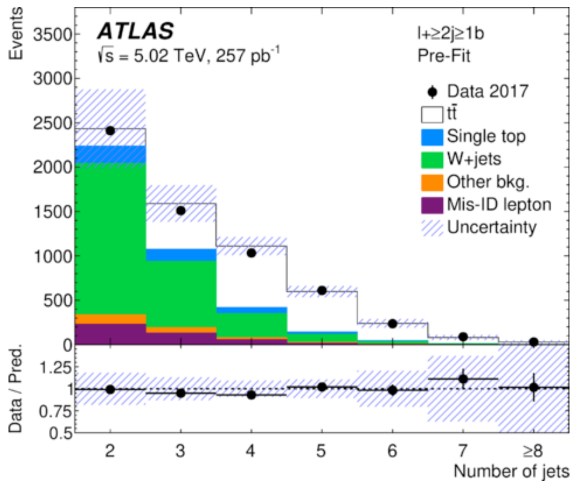

Inclusive $t\bar{t}$ cross-section at 5.02 TeV

Comparison with theory and PDF contraints

JHEP04 (2022) 144

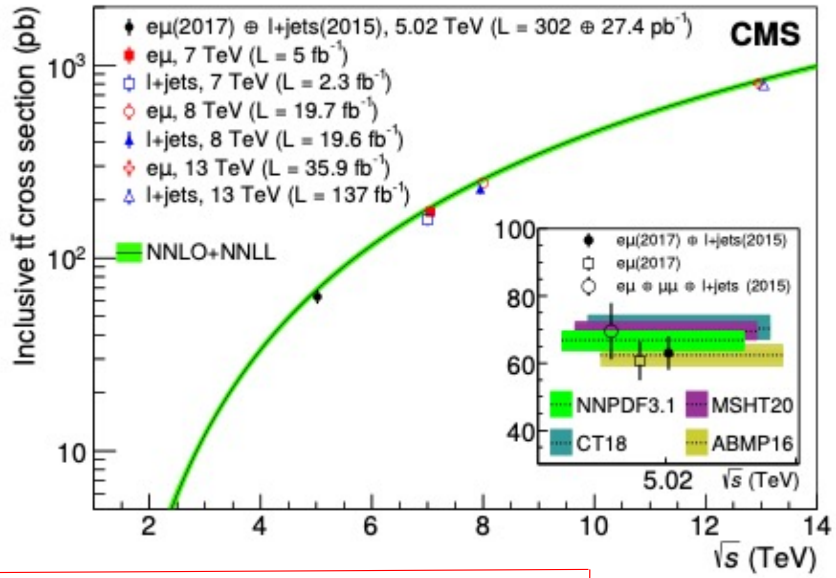

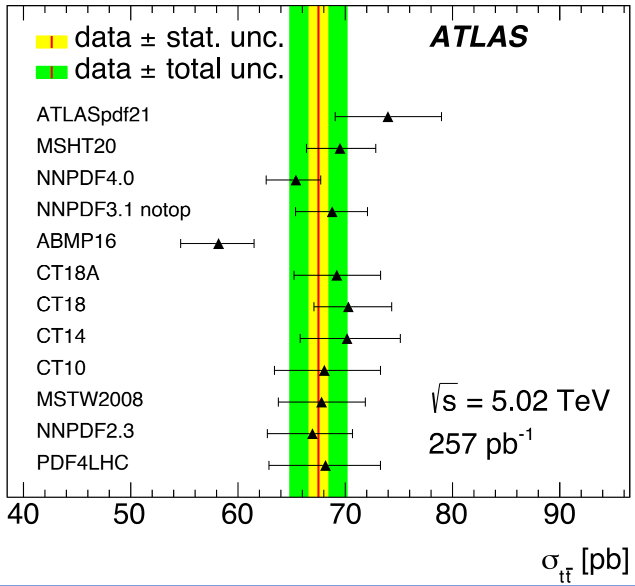

arXiv:2207.01354

Impressive agreement with the QCD prediction over pp collision energies from 5 to 13 TeV and an order of magnitude of x-section

$\sigma_{tt}(\sqrt{s})$ helps also to constrain PDFs

The 5 TeV ATLAS result reduces the uncertainty on *xg(x)* by 5% at x=0.1.

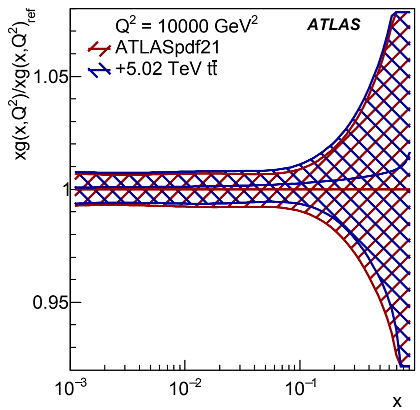

CMS-PAS-TOP-20-006

Differential dileptonic $t\bar{t}$ + jets cross-sections at 13 TeV

- Full Run2 138 fb^{-1}
- Extended pT range, more kinematic bins
- Experimental uncertainties ~1/2 of 36 fb^{-1} analysis (Eur. Phys. J. C(2020)80:658) (better JES, in situ backgrounds, more statistics)
- Unfold to both parton and particle level

NLO QCD models predict somewhat harder top p_T spectra, and slightly more central, than seen in data (same effect seen in lepton spectra)

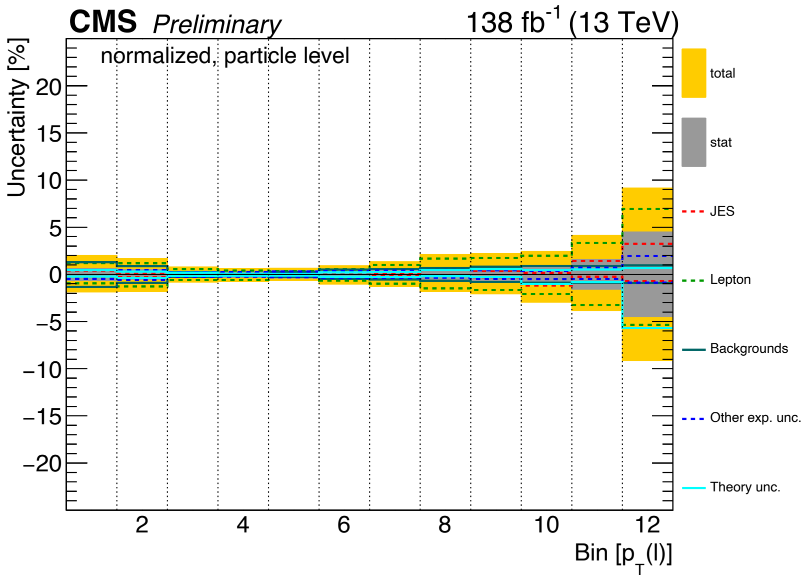

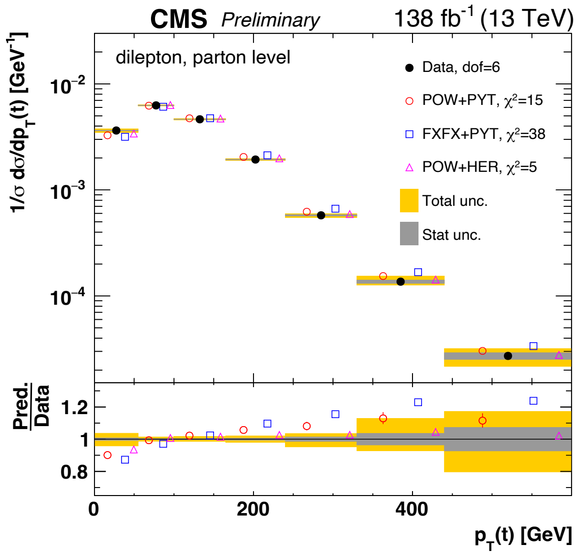

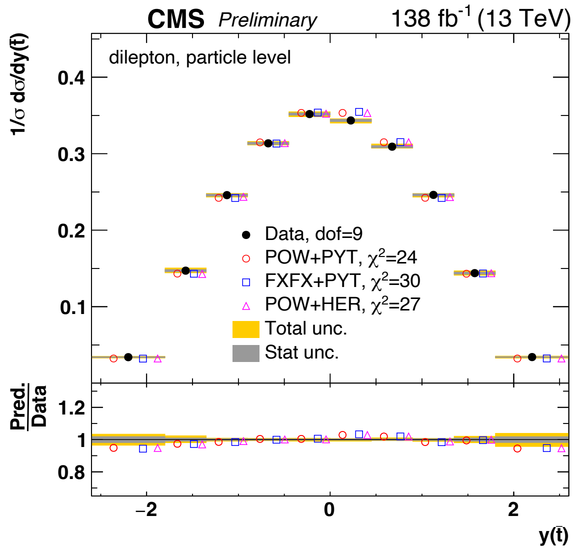

[CMS-PAS-TOP-20-006](CMS-PAS-TOP-20-006)

Differential dileptonic $t\bar{t}$ + jets cross-sections

- NNLO corrections help, but do not remove all tensions

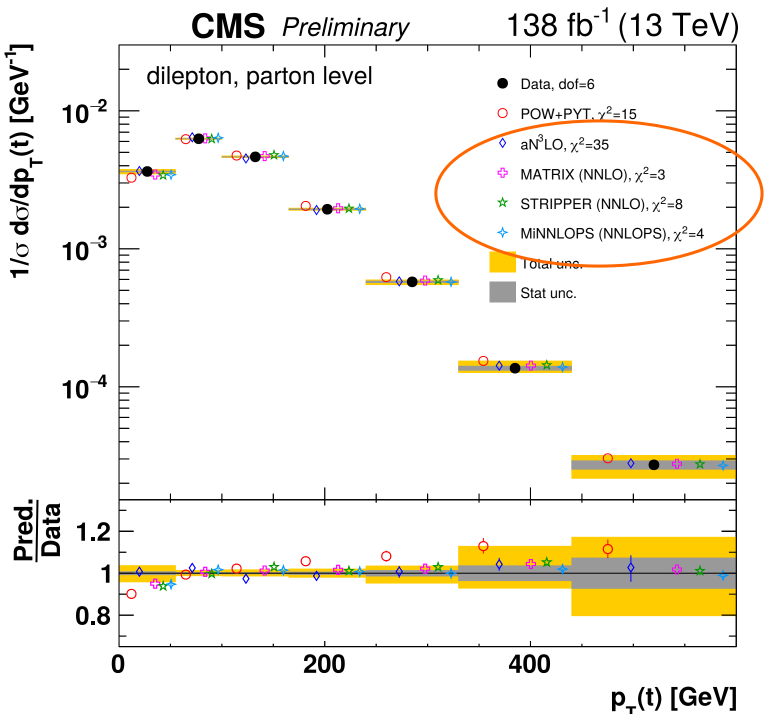

Double and triple differential distributions probe the tensions with QCD models in detail. No model describe all these data well within experimental uncertainties.

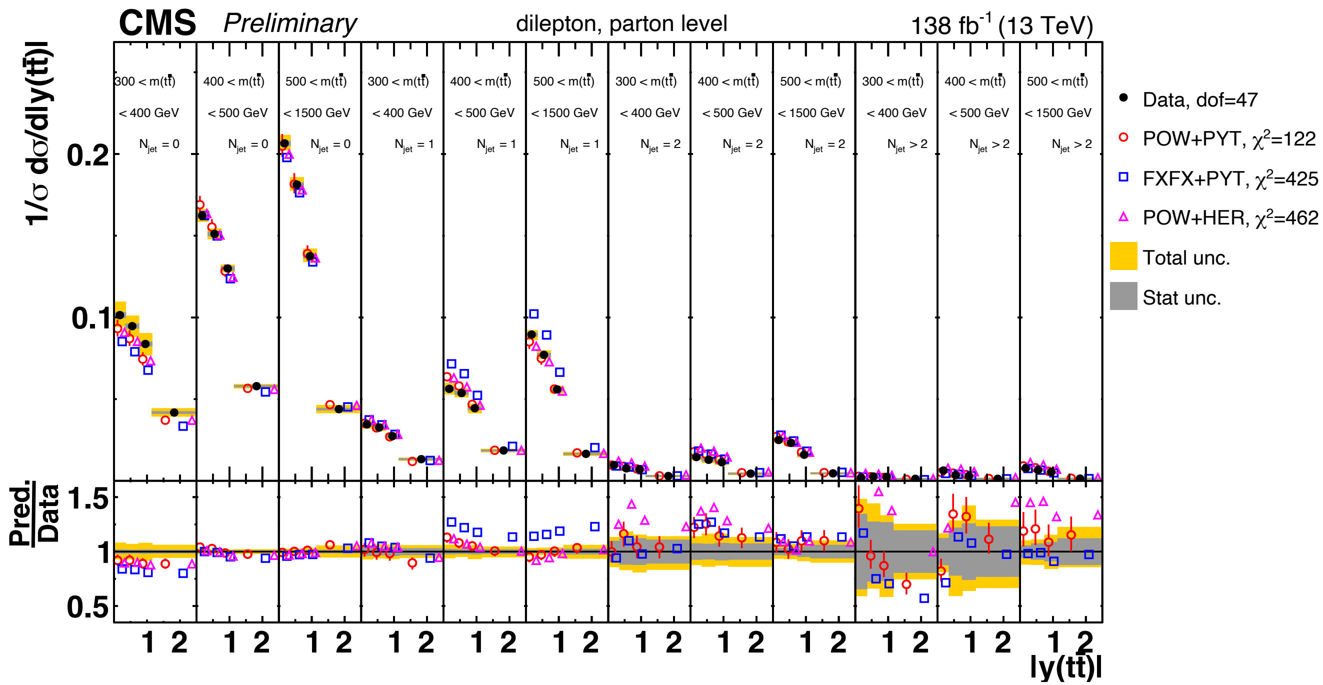

The largest tension is in the number of additional jets, especially for high m_{tt}, in the case of FXFX+PYT and POW+HER.

ATLAS-CONF-2022-061

Differential dileptonic $t\bar{t}$ cross-sections at 13 TeV

- ATLAS has measured (double) differential cross-sections for 8 kinematic variables in the $e\mu$ channel.
- Same double tagging technique as in slide 3, but solved for each kinematic bin using the full Run2 sample.
- The largest uncertainty is luminosity overall, and Wt background at high p_T^{lept}. *Typically 1-2% per bin in norm. distr.*
- The results are compared with various models. None are compatible with all data within exp. uncertainties - e.g:

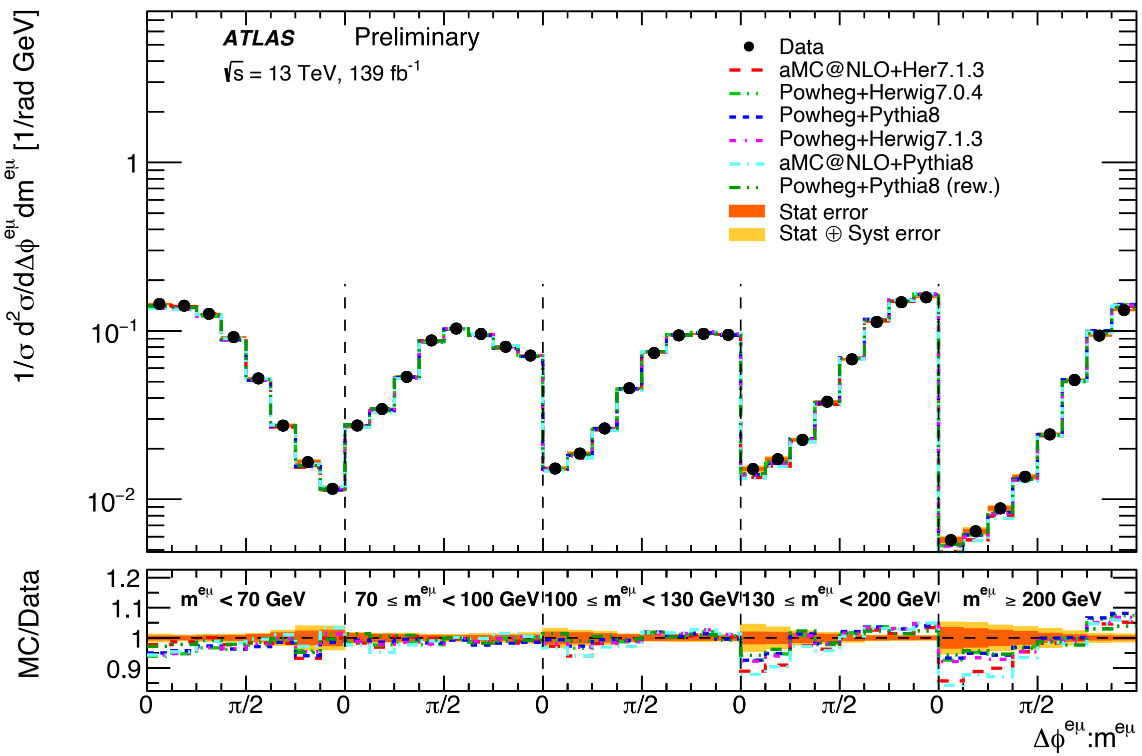

- Again a softer p_T^{lept} spectrum is observed than predicted by PowHeg+Pythia8 and other NLO gen.

However, reweighing PH+P8 to reproduce the NNLO p_T^{top} distribution reduces the χ^2 from 196 to 51 (for 8 dof).

- The normalised distributions of $\Delta\phi^{e\mu}$ vs $m^{e\mu}$ produces $\chi^2/ndof = 374/38$ for PowHeg+Pythia8.

However, by reweighing as above, or by increasing radiation, the χ^2 decreases by more than a factor two.

The inclusive cross-section is measured to be

$$\sigma_{t\bar{t}} = 836 \pm 1(stat) \pm 12(syst) \pm 16(lum + E_{cms})$$

2.4% uncertainty

Inclusive cross-section using lepton+jets @ 13 TeV

- Select 7M events with one lepton and at least four jets from the Run2 sample
- Three signal regions with different n_{jet} and n_{btag} selected with purities ~90%
- Use a discriminating variable in each region and a profile likelihood fit to determine the signal fraction.

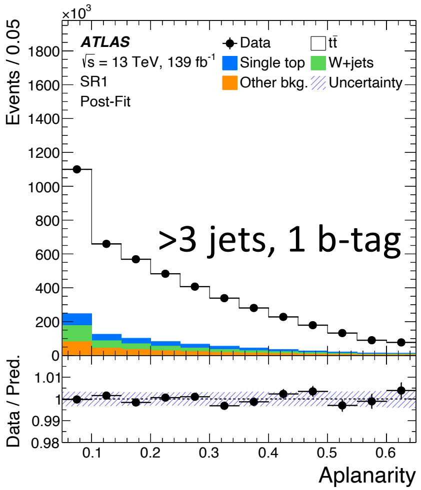

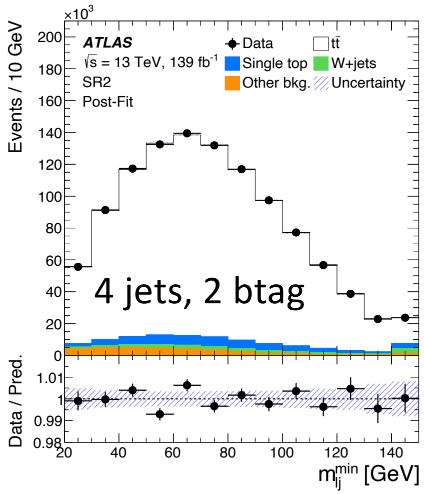

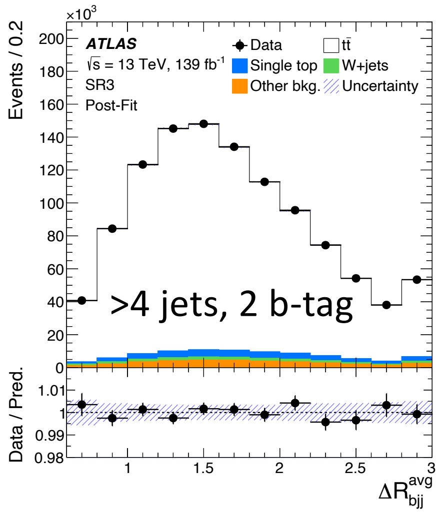

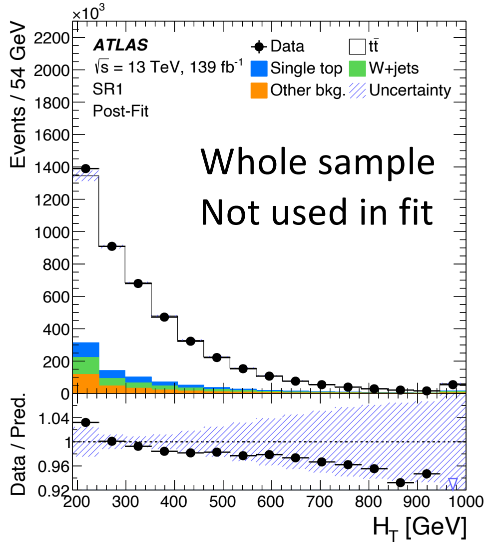

PLB810(2020)135797

$$\sigma_{\text{inc}} = 830 \pm 0.4\ (\text{stat.}) \pm 36\ (\text{syst.}) \pm 14\ (\text{lumi.})\ \text{pb}$$ 4.6% uncertainty

Factor of two larger uncertainty than the ATLAS $e\mu$ result of 836 ± 20 pb.

Both agree with NNLO QCD prediction: $\sigma_{t\bar{t},pred} = 832^{+20}_{-29}(scale) \pm 23(m_t) \pm 35(PDF + \alpha_S)$ ATLAS ref

Differential cross-sections using lepton+jets @ 13 TeV

- One lepton and at least four jets, including boosted topologies
- Reconstructs top quarks in four event classes -> parton level x-sections
- The high statistics allows for differential measurements in expanded phase-space, as compared with the dilepton channel.
- Double differential x-sections show details about model tensions. For example:

Phys.Rev.D 104, 092013

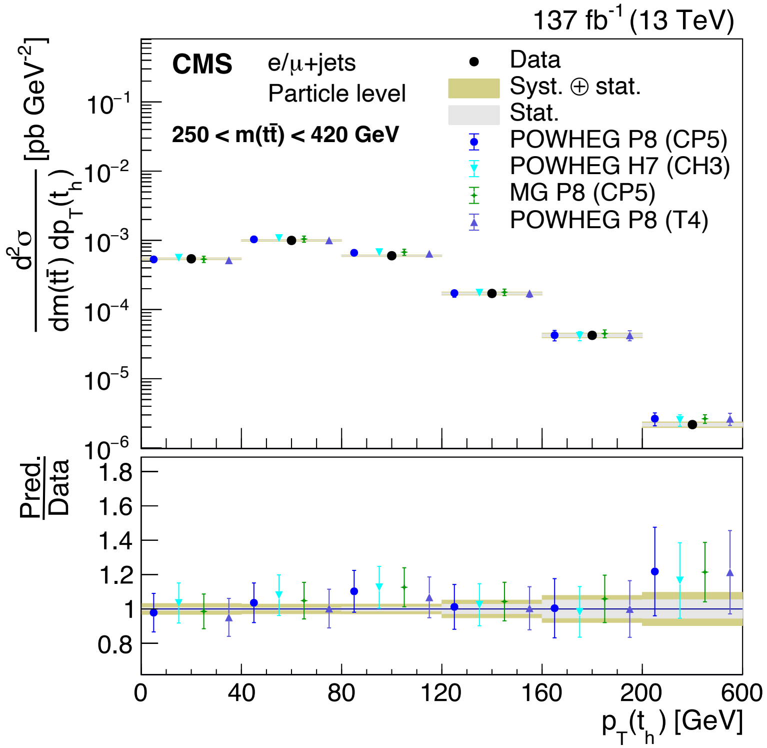

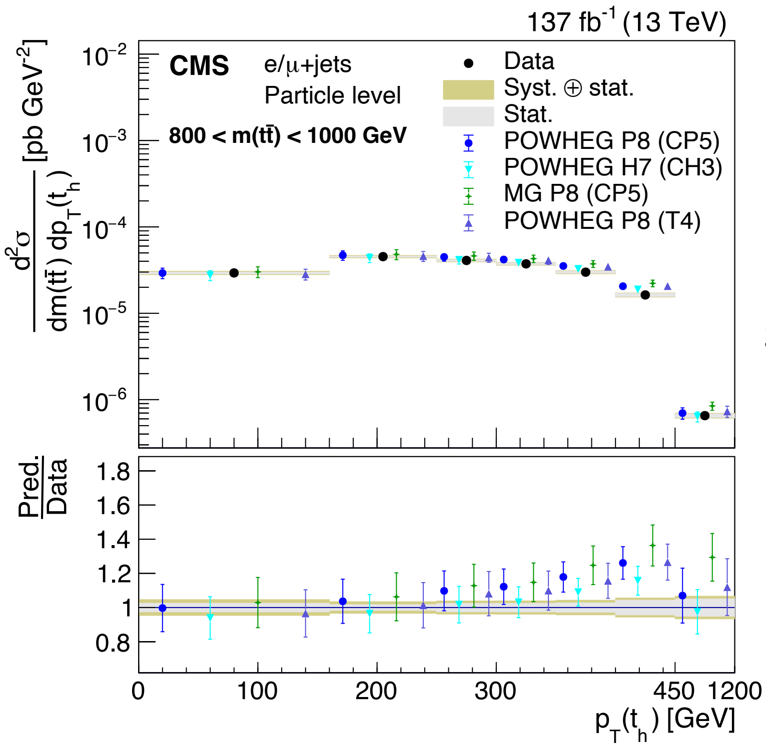

P_T^t spectra again softer than predicted by the NLO models

But mainly at high $m(t\bar{t})$

Differential cross-sections using lepton+jets @ 13 TeV

- MATRIX (NNLO calc.) predicts a softer top p_T spectrum than the NLO models, and has smaller scale dependence. However, still some tensions remain.

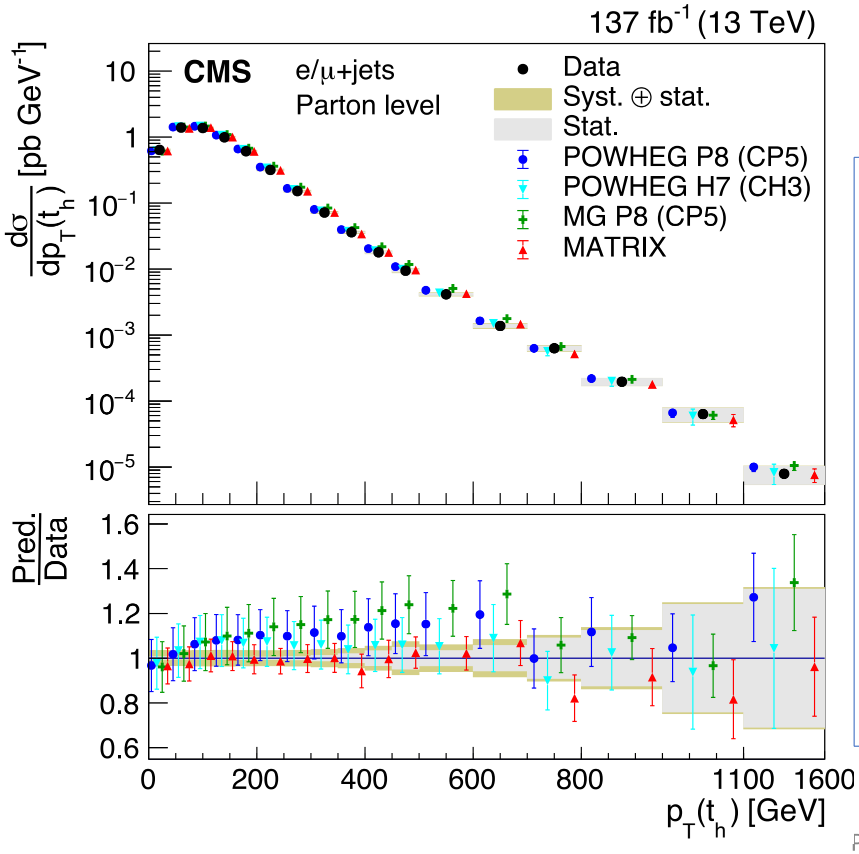

Models also have problems with N_{jets} and other variables related to radiation, see also next slide.

The inclusive cross-section is found to be:

$$\sigma_{t\bar{t}} = 791 \pm 1\,(\text{stat}) \pm 21\,(\text{syst}) \pm 14\,(\text{lumi})\ \text{pb}$$

With an uncertainty of 3.2%, the most precise result in this channel.

Agrees with ATLAS and with the MATRIX pred.:

$$\sigma_{t\bar{t}}^{pred} = 797^{+39}_{-51}\,(\text{scale}) \pm 39\,(\text{PDF})\ \text{pb}$$

Phys.Rev.D 104, 092013

Differential cross-sections using lepton+jets @ 13 TeV

- Select l + b-jet + top-tagged wide jet -> 75743 events , >95% $t\bar{t}$
- In situ JES calibration plus improved top- and b-tagging methods reduce jet systematics by factor 2 relative to the earlier analysis based on 36 fb^{-1} (Phys.Rev.D 98 (2018) 012003)

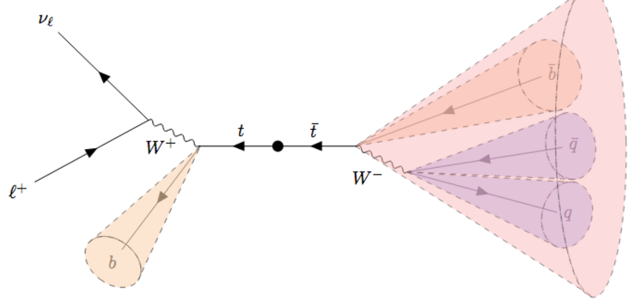

JHEP06(2022)063

Additional jet p_T's are generally not well described by QCD models

Neither are their azimuthal distances to the "hadronic top"

However, reweighing to the NNLO top p_T dist. helps

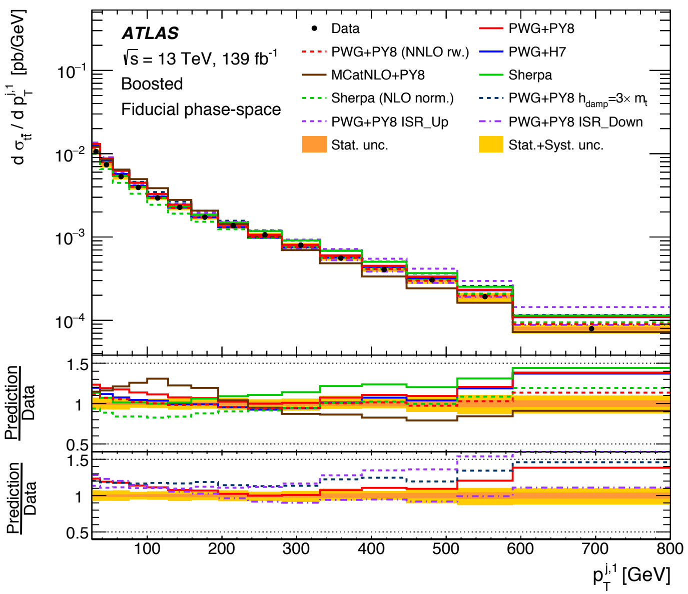

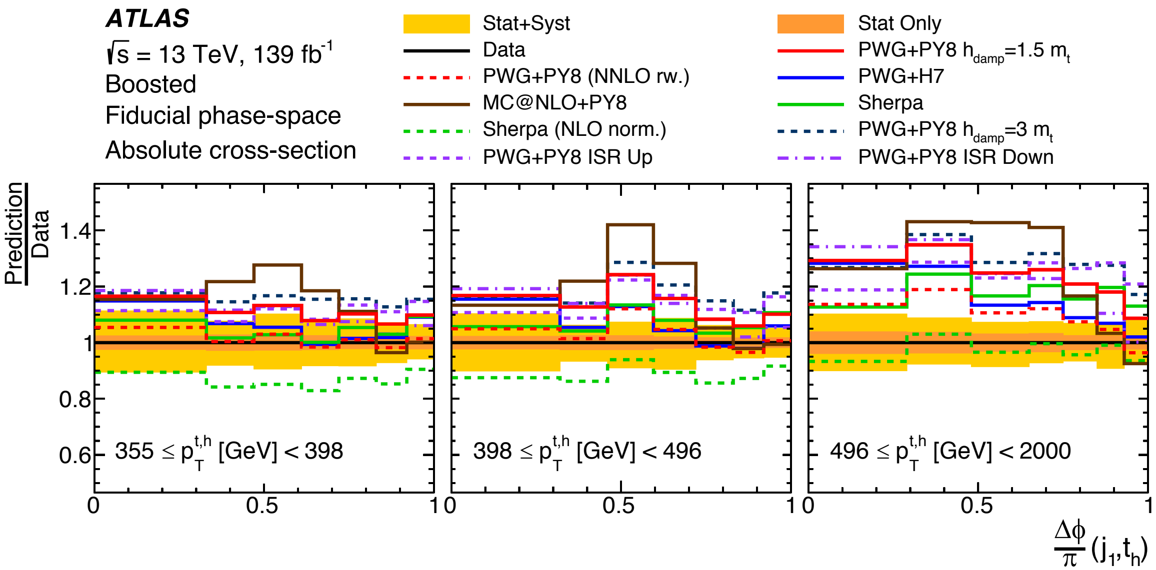

Limits also set on Wilson coef.

See Jonathan Wilsons talk

Fiducial cross-section using ”all jets” @ 13 TeV

- Hadronic top pair decays are identified in their boosted topology, yielding 17261 events with p_T(wide jets)>500, 350 GeV

- 81% $t\bar{t}$, 15% multijet (as estimated from data)

- Unfolded to fiducial phase-space (both parton and particle level)

- NNLO+NNLL model (MATRIX) reproduces the fiducial cross-section better than the NLO models. Reweighing the NLO to NNLO p_T(top) approaches the NNLO result.

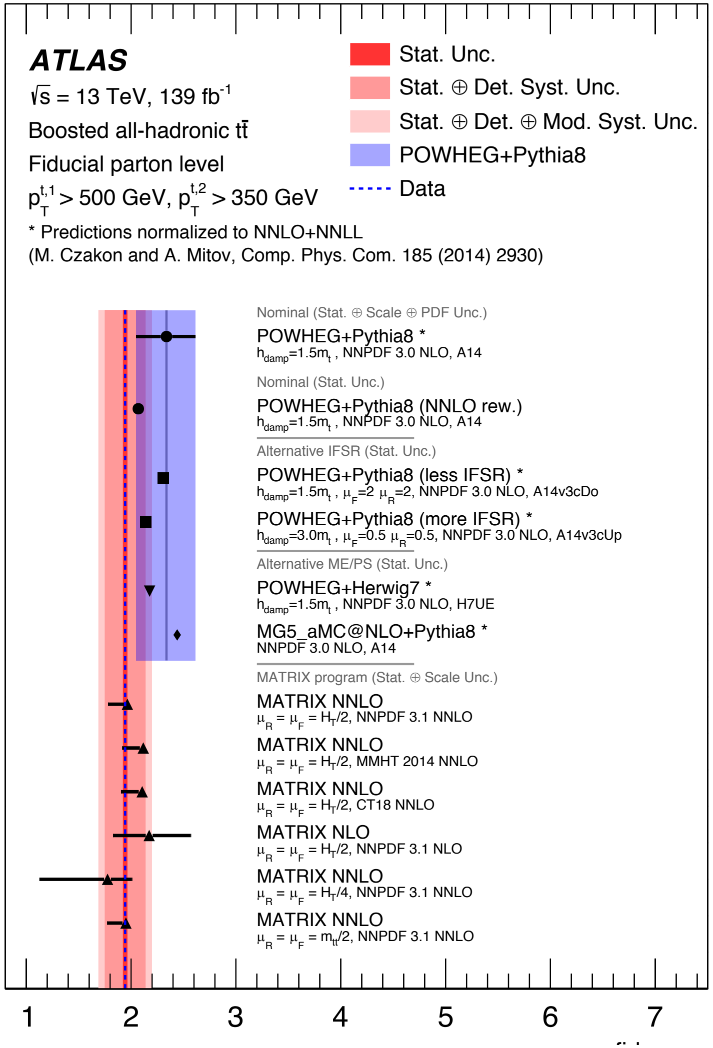

arXiv:2205.02817

Differential cross-sections using ”all jets” @ 13 TeV

- General agreement between data and PWG+Py8 (especially for the variant with more radiation)
- However, especially MG5_aMC@NLO and PWG+H7 struggle with radiation (variables like $p_T^{tt}, \Delta\varphi^{tt}$,N_{jet}) but less so at parton level than at particle level.

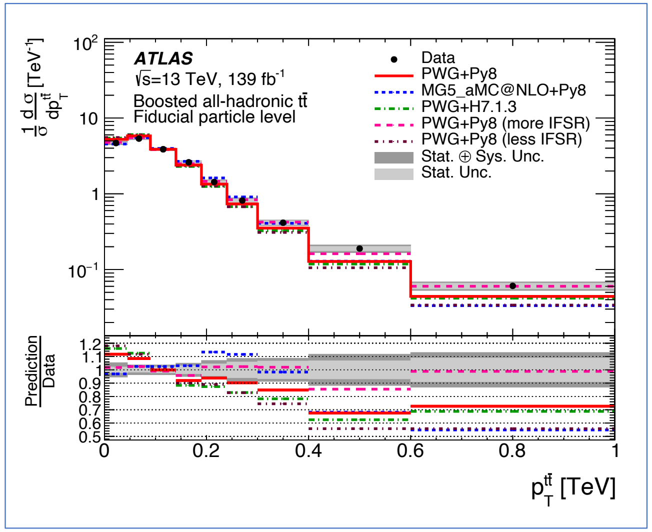

arXiv:2205.02817

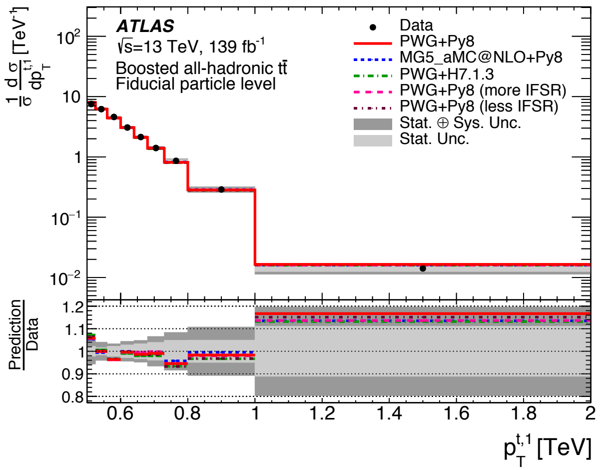

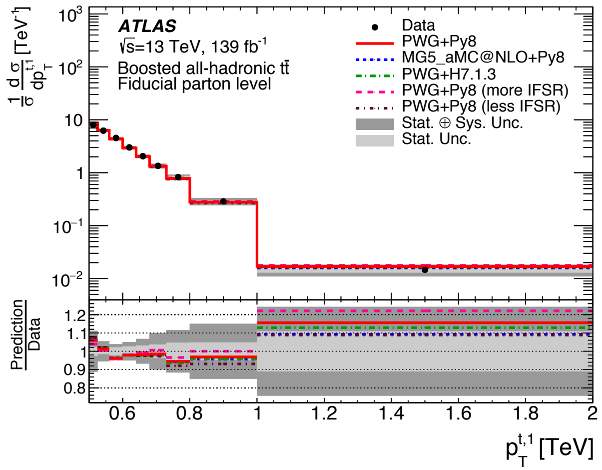

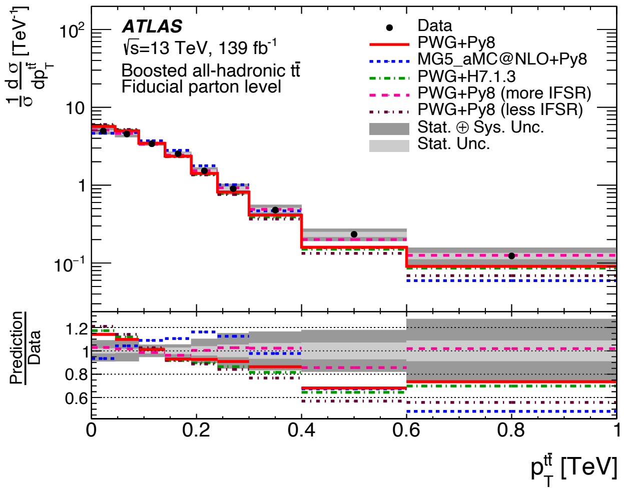

Limits on Wilson coefficients are also set. See Jonathan Wilsons talk.

Summary

- Precise inclusive top-pair cross-sections have been measured at 13 TeV
  Uncertainty examples are 2.4% (ATLAS $e\mu$ channel) and 3.2% (CMS l+jets), dominated by luminosity and theory.

- Legacy combination of Run1 inclusive cross-sections at 7 and 8 TeV and new results at 5.02 TeV. Excellent agreement with NNLO+NNLL calculations over 5-13 TeV collision energies.

- Differential (plus double- and triple-differential) cross-sections at 13 TeV measured using the large Run2 data sample.
  Uncertainties dominated by systematics (except at very large p_T).
  No model describes the data perfectly, especially regarding p_T and N_{jet} (see also Rene Poncelet's talk), but NNLO calculations describes the measured p_T^{top} distribution better than the NLO generators.

- These measurements can be used to determine m_t, α_S and the PDFs (see Matteo Defranchis's talk), as well as to constrain EFT terms (see Jonathan Wilsons talk).

Backup slides

Charge asymmetry

Higher order corrections to $t\bar{t}$ production from $q\bar{q}$ annihilation is expected to lead to a small asymmetry

$A_C = \frac{N(\Delta|y|>0)-N(\Delta|y|<0)}{N(\Delta|y|>0)+N(\Delta|y|<0)} = (0.94^{+0.05}_{-0.07})\%$ with $\Delta|y| = |y_t| - |y_{\bar{t}}|$ (M.Czakon et al., PRD98(2018)014003)

CMS has measured it in the l+jets channel using full Run2 for highly boosted top quarks, ensured by the selection

$$m_{t\bar{t}} > 750\ GeV$$

The measurement yields $A_C = (0.69^{+0.65}_{-0.69})\%$ in agreement with the expectation

Statistics, scale variations, JES and PDFs are the largest sources of uncertainty

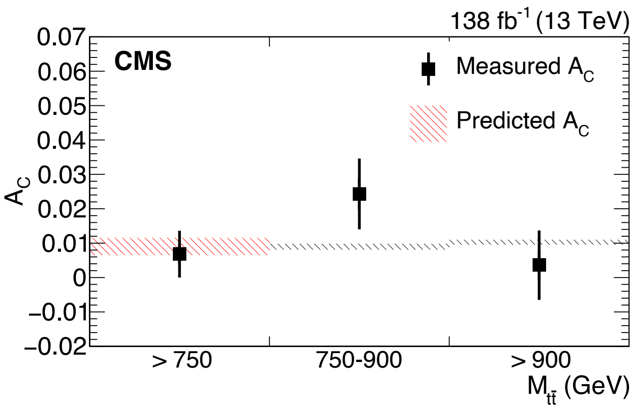

arXiv:2208.02751

ATLAS has measured the asymmetry in sample of $t\bar{t}\gamma$ events. Here, however, the asymmetry is expected to have a small negative value due to QED ISR-FSR interference (-1.4% in MadGraph5).
The value measured by ATLAS in Run2 is $A_C(t\bar{t}\gamma) = (-0.6 \pm 3.0)\%$ in agreement with the prediction.

ATLAS-CONF-2022-049

The largest uncertainties

- The luminosity contributes the largest uncertainty on the inclusive fiducial cross-section in the dilepton channel.

- Differences in models due to higher orders, ME-shower matching, hadronization dominates its extrapolation to full phase-space.

- At high p_T, the dominant error is Wt background in the $e\mu$ channel (especially amplitude interference).

- The jet energy scale contributes the largest single systematic error in the lepton+jet channel and the all-jet channel.

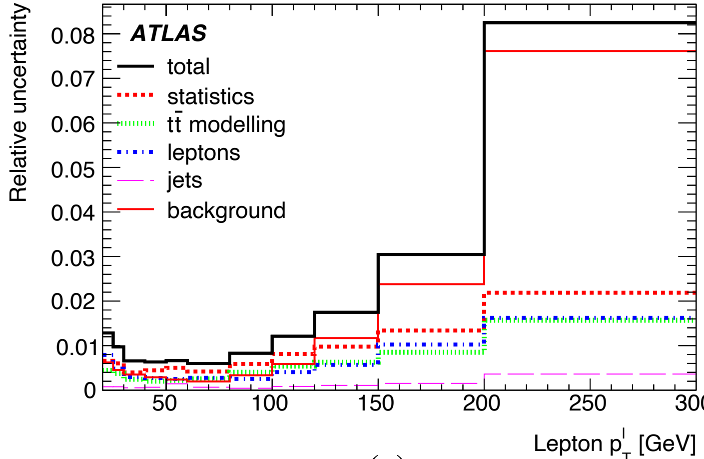

(a)

Eur.Phys.J.C80(2020)528

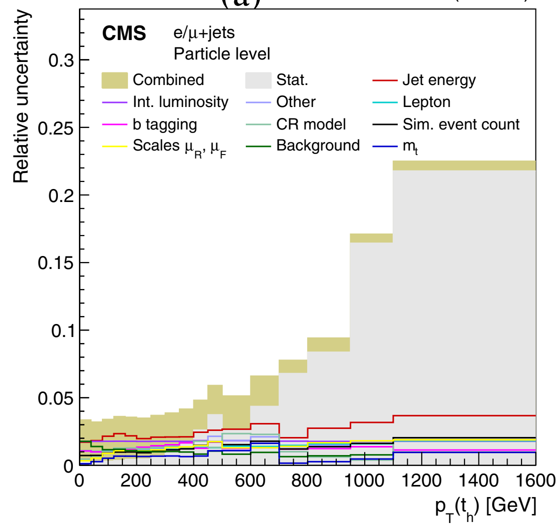

Phys.Rev.D 104, 092013

Differential dileptonic $t\bar{t}$ + jets cross-sections

Cross section variables	dof	χ^2 POW+PYT	χ^2 POW+HER	χ^2 FXFX+PYT
$[\lvert y(\mathrm{t})\rvert,\ p_{\mathrm{T}}(\mathrm{t})]$	16	48	30	75
$[m(\mathrm{t\bar{t}}),\ p_{\mathrm{T}}(\mathrm{t})]$	9	93	42	156
$[p_{\mathrm{T}}(\mathrm{t}),\ p_{\mathrm{T}}(\mathrm{t\bar{t}})]$	16	50	87	72
$[m(\mathrm{t\bar{t}}),\ \lvert y(\mathrm{t\bar{t}})\rvert]$	16	72	65	67
$[\lvert y(\mathrm{t\bar{t}})\rvert,\ p_{\mathrm{T}}(\mathrm{t\bar{t}})]$	16	32	71	37
$[m(\mathrm{t\bar{t}}),\ p_{\mathrm{T}}(\mathrm{t\bar{t}})]$	16	68	115	77
$[p_{\mathrm{T}}(\mathrm{t\bar{t}}),\ m(\mathrm{t\bar{t}}),\ y(\mathrm{t\bar{t}})]$	48	102	140	119
$[m(\mathrm{t\bar{t}}),\ \lvert y(\mathrm{t})\rvert]$	16	67	49	84
$[m(\mathrm{t\bar{t}}),\ \lvert\Delta\eta(\mathrm{t},\mathrm{\bar{t}})\rvert]$	12	182	126	236
$[m(\mathrm{t\bar{t}}),\ \lvert\Delta\phi(\mathrm{t},\mathrm{\bar{t}})\rvert]$	12	82	94	50

Cross section variables	dof	χ^2 POW+PYT	χ^2 POW+HER	χ^2 FXFX+PYT
$N_{\mathrm{jet}}(p_{\mathrm{T}} > 40\,\mathrm{GeV})$	6	7	258	288
$N_{\mathrm{jet}}(p_{\mathrm{T}} > 100\,\mathrm{GeV})$	5	41	77	46
$[N_{\mathrm{jet}},\ p_{\mathrm{T}}(\mathrm{t})]$	9	31	137	163
$[N_{\mathrm{jet}},\ \lvert y(\mathrm{t})\rvert]$	12	42	85	131
$[N_{\mathrm{jet}},\ p_{\mathrm{T}}(\mathrm{t\bar{t}})]$	12	58	93	192
$[N_{\mathrm{jet}},\ m(\mathrm{t\bar{t}})]$	12	62	154	177
$[N_{\mathrm{jet}},\ \lvert y(\mathrm{t\bar{t}})\rvert]$	12	14	61	122
$[N_{\mathrm{jet}},\ \Delta\eta(\mathrm{t},\mathrm{\bar{t}})]$	9	94	144	194
$[N_{\mathrm{jet}}^{0,1+},\ m(\mathrm{t\bar{t}}),\ \lvert y(\mathrm{t\bar{t}})\rvert]$	24	54	93	75
$[N_{\mathrm{jet}}^{0,1,2+},\ m(\mathrm{t\bar{t}}),\ \lvert y(\mathrm{t\bar{t}})\rvert]$	36	93	215	223
$[N_{\mathrm{jet}}^{0,1,2,3+},\ m(\mathrm{t\bar{t}}),\ \lvert y(\mathrm{t\bar{t}})\rvert]$	48	135	471	445

[Phys.Rev.D 104, 092013](#)

Cross section variables	dof	χ^2 POW+PYT	χ^2 POW+HER	χ^2 FXFX+PYT
$p_{\mathrm{T}}(\ell)$	12	32	21	62
$p_{\mathrm{T}}(\ell)$ trailing $/\ p_{\mathrm{T}}(\ell)$ leading	10	16	7	27
$p_{\mathrm{T}}(\ell)/p_{\mathrm{T}}(\mathrm{\bar{t}})$	5	20	14	28
$p_{\mathrm{T}}(\mathrm{b})$ leading	10	6	8	31
$p_{\mathrm{T}}(\mathrm{b})$ trailing	7	7	7	26
$(p_{\mathrm{T}}(\mathrm{b}) + p_{\mathrm{T}}(\mathrm{\bar{b}}))/(p_{\mathrm{T}}(\mathrm{t}) + p_{\mathrm{T}}(\mathrm{\bar{t}}))$	4	24	21	30
$m(\ell\bar{\ell})$	12	31	23	29
$m(\mathrm{b\bar{b}})$	7	21	15	17
$m(\ell\bar{\ell}\mathrm{b\bar{b}})$	19	36	27	30
$p_{\mathrm{T}}(\ell\bar{\ell})$	9	4	10	17
$\lvert\eta(\ell\bar{\ell})\rvert$	14	16	12	22
$[\lvert\eta(\ell\bar{\ell})\rvert,\ m(\ell\bar{\ell})]$	24	55	35	76
$[\lvert\eta(\ell\bar{\ell})\rvert,\ p_{\mathrm{T}}(\ell\bar{\ell})]$	20	30	24	84
$[p_{\mathrm{T}}(\ell\bar{\ell}),\ m(\ell\bar{\ell})]$	30	50	52	88

Inclusive dileptonic $t\bar{t}$ cross-section

Source of uncertainty	$\Delta\sigma^{\text{fid}}_{t\bar{t}}/\sigma^{\text{fid}}_{t\bar{t}}$ (%)	$\Delta\sigma_{t\bar{t}}/\sigma_{t\bar{t}}$ (%)
Data statistics	0.15	0.15
MC statistics	0.04	0.04
Matrix Element	0.12	0.17
h_{damp} variation	0.01	0.01
Parton shower	0.08	0.22
$t\bar{t}$ + Heavy Flavour	0.34	0.34
top p_{T} reweighting	0.19	0.58
Parton distribution functions	0.04	0.43
Initial state radiation	0.11	0.37
Final state radiation	0.29	0.35
Electron energy scale	0.10	0.10
Electron efficiency	0.37	0.37
Electron isolation (in situ)	0.51	0.51
Muon momentum scale	0.13	0.13
Muon reconstruction efficiency	0.35	0.35
Muon isolation (in situ)	0.33	0.33
Lepton trigger efficiency	0.05	0.05
Vertex association efficiency	0.03	0.03
Jet energy scale/resolution	0.10	0.10
b-tagging efficiency	0.07	0.07
$t\bar{t}$/Wt interference	0.37	0.37
Wt cross-section	0.52	0.52
Diboson background	0.18	0.18
$t\bar{t}$ V + $t\bar{t}$ H	0.03	0.03
Z+jets background	0.05	0.05
Misidentified leptons	0.32	0.32
Beam energy	0.23	0.23
Luminosity	1.90	1.90
Total uncertainty	2.3	2.4

ATLAS-CONF-2022-061

Inclusive cross-section using lepton+jets @ 13 TeV

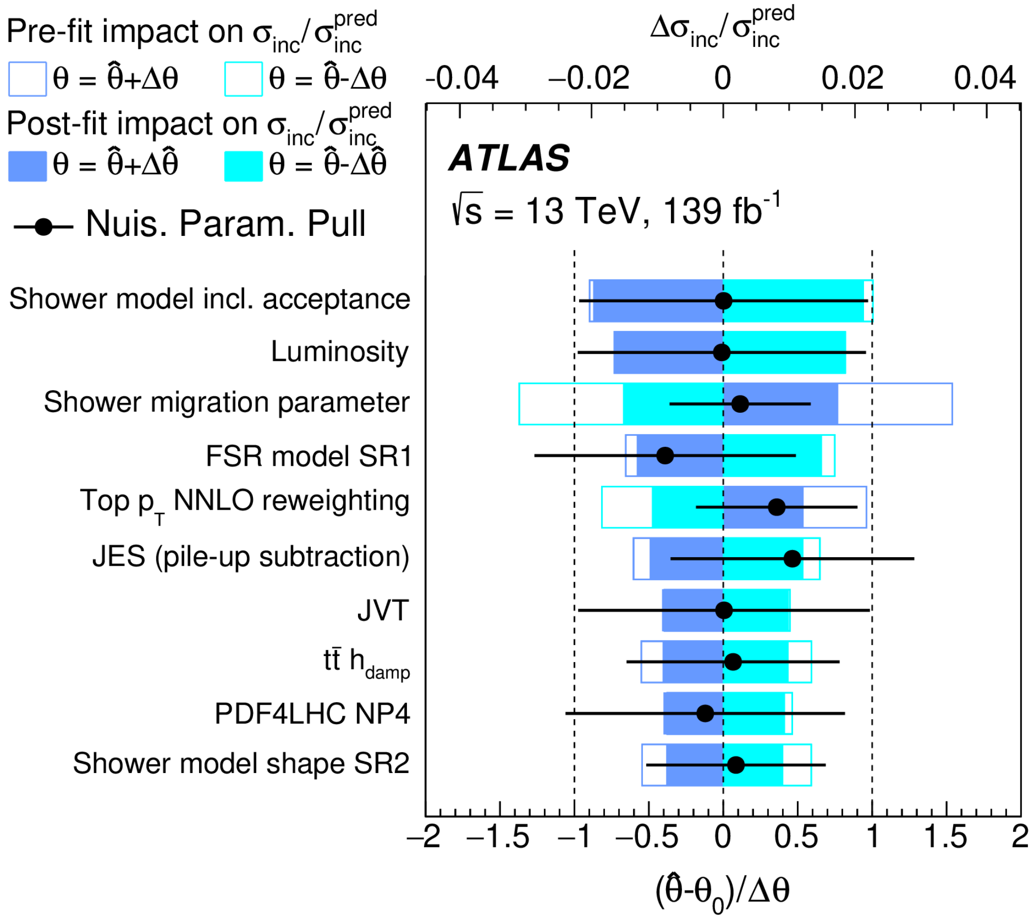

PLB810(2020)135797

Differential cross-sections using lepton+jets @ 13 TeV

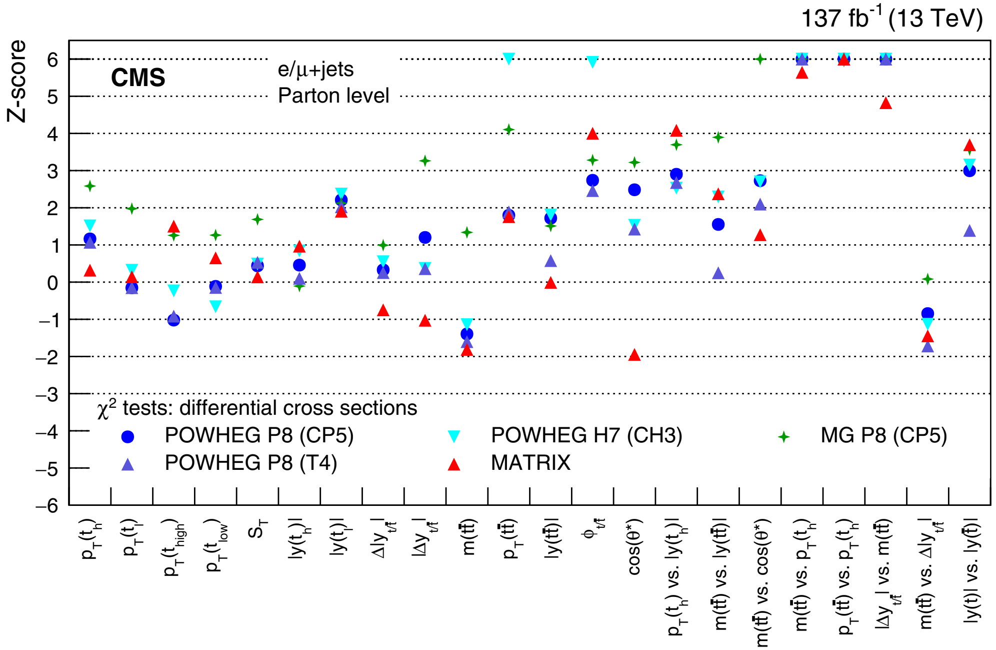

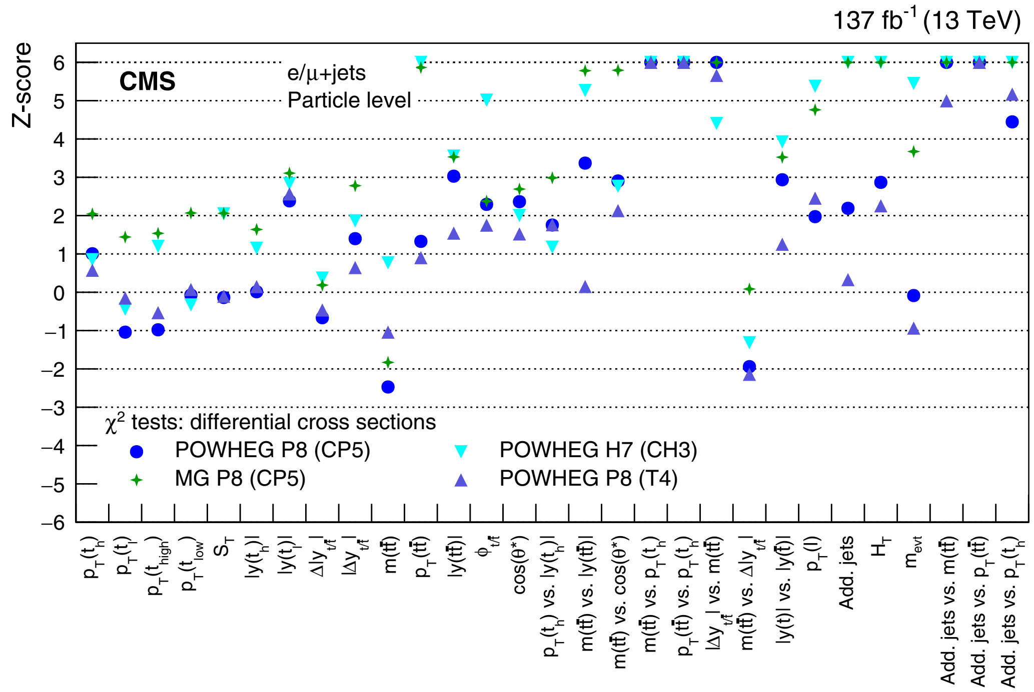

Phys.Rev.D 104, 092013

Differential cross-sections using lepton+jets @ 13 TeV

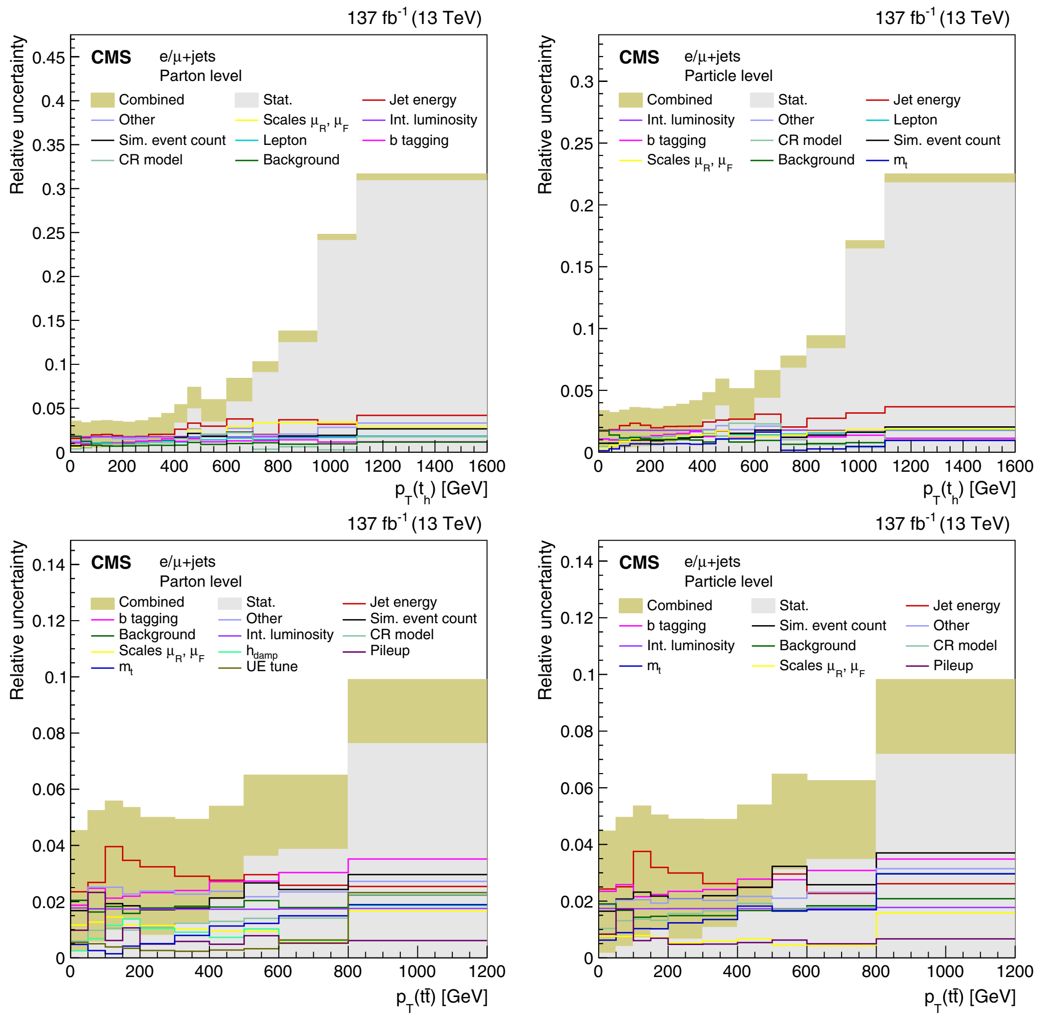

Phys.Rev.D 104, 092013

Differential cross-sections using lepton+jets @ 13 TeV

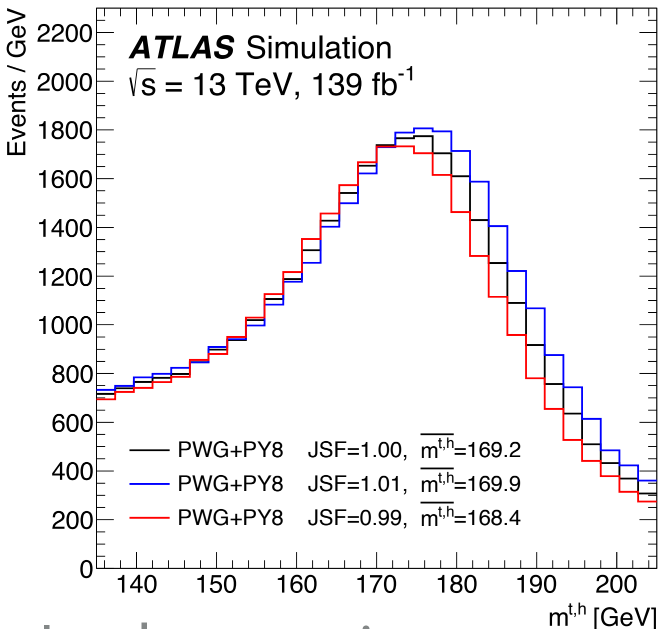

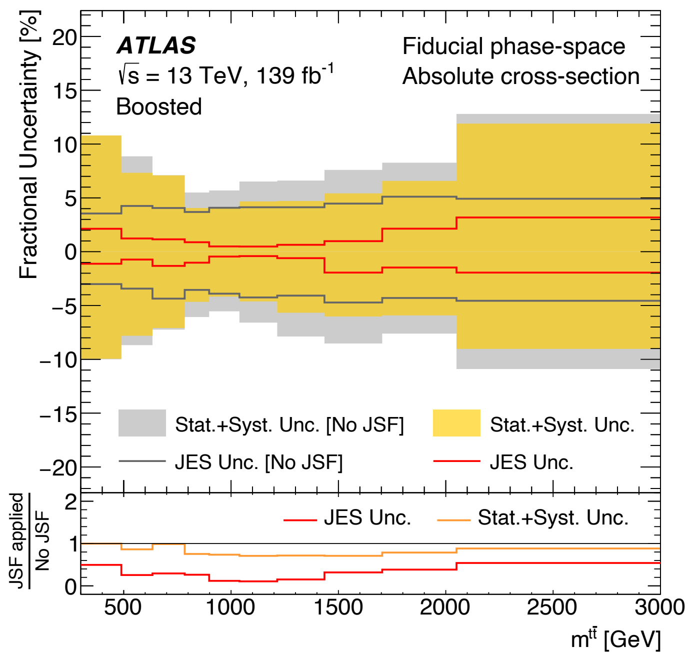

JHEP06(2022)063

Perform extra JSF calibration using a linear relation with the mean measured hadronic top mass. Limited by the top mass uncertainty.

Significantly reduces a leading uncertainty in most bins

Differential cross-sections using lepton+jets @ 13 TeV

Observable	PWG+PY8		PWG+PY8(ISR Down)		PWG+PY8(ISR Up)		PWG+PY8($h_{\mathrm{damp}} = 3m_t$)		SHERPA		SHERPA (NLO norm.)	
	χ^2/NDF	p-value	χ^2/NDF	p-value	χ^2/NDF	p-value	χ^2/NDF	p-value	χ^2/NDF	p-value	χ^2/NDF	p-value
$p_{\mathrm{T}}^{t,h}$	26/8	<0.01	26/8	<0.01	25/8	<0.01	36/8	<0.01	12/8	0.15	11/8	0.19
$p_{\mathrm{T}}^{t,\ell}$	78/8	<0.01	144/8	<0.01	20/8	0.01	50/8	<0.01	12/8	0.13	11/8	0.22
$p_{\mathrm{T}}^{t\bar{t}}$	162/7	<0.01	243/7	<0.01	340/7	<0.01	108/7	<0.01	70/7	<0.01	57/7	<0.01
$H_{\mathrm{T}}^{t\bar{t}+\mathrm{jets}}$	36/7	<0.01	38/7	<0.01	96/7	<0.01	52/7	<0.01	39/7	<0.01	34/7	<0.01
$H_{\mathrm{T}}^{t\bar{t}}$	86/10	<0.01	119/10	<0.01	46/10	<0.01	72/10	<0.01	28/10	<0.01	22/10	0.01
$\lvert y^{t,h}\rvert$	47/17	<0.01	46/17	<0.01	46/17	<0.01	55/17	<0.01	25/17	0.10	20/17	0.29
$\lvert y^{t,\ell}\rvert$	40/14	<0.01	45/14	<0.01	34/14	<0.01	45/14	<0.01	24/14	0.05	18/14	0.19
$\lvert y^{t\bar{t}}\rvert$	30/10	<0.01	32/10	<0.01	23/10	<0.01	35/10	<0.01	22/10	0.02	20/10	0.03
$m^{t\bar{t}}$	52/10	<0.01	78/10	<0.01	75/10	<0.01	53/10	<0.01	31/10	<0.01	25/10	<0.01
$p_{\mathrm{T}}^{j,1}$	115/15	<0.01	136/15	<0.01	272/15	<0.01	74/15	<0.01	140/15	<0.01	98/15	<0.01
$p_{\mathrm{T}}^{j,2}$	46/9	<0.01	12/9	0.23	196/9	<0.01	81/9	<0.01	41/9	<0.01	19/9	0.02
N^j	32/5	<0.01	51/5	<0.01	27/5	<0.01	41/5	<0.01	23/5	<0.01	16/5	<0.01
$\Delta\phi(j_1, t_h)$	17/9	0.05	34/9	<0.01	22/9	<0.01	23/9	<0.01	10/9	0.38	11/9	0.25
$\Delta\phi(j_2, t_h)$	8/9	0.56	7/9	0.67	22/9	0.01	19/9	0.03	6/9	0.74	3/9	0.96
$\Delta\phi(b_\ell, t_h)$	95/13	<0.01	116/13	<0.01	294/13	<0.01	119/13	<0.01	51/13	<0.01	28/13	0.01
$\Delta\phi(t_h, t_\ell)$	111/5	<0.01	164/5	<0.01	207/5	<0.01	79/5	<0.01	36/5	<0.01	39/5	<0.01
$\Delta\phi(j_1, j_2)$	24/11	0.01	17/11	0.12	41/11	<0.01	38/11	<0.01	26/11	<0.01	20/11	0.05
$m(j_1, t_h)$	50/12	<0.01	111/12	<0.01	93/12	<0.01	43/12	<0.01	65/12	<0.01	40/12	<0.01
$p_{\mathrm{T}}^{j,1}$ vs N^j	355/21	<0.01	495/21	<0.01	488/21	<0.01	254/21	<0.01	193/21	<0.01	137/21	<0.01
$p_{\mathrm{T}}^{j,1}$ vs $p_{\mathrm{T}}^{t,h}$	115/17	<0.01	192/17	<0.01	256/17	<0.01	87/17	<0.01	133/17	<0.01	87/17	<0.01
$\Delta\phi(j_1, t_h)$ vs $p_{\mathrm{T}}^{t,h}$	69/21	<0.01	104/21	<0.01	56/21	<0.01	73/21	<0.01	42/21	<0.01	32/21	0.06
$\Delta\phi(j_1, t_h)$ vs N^j	109/19	<0.01	201/19	<0.01	66/19	<0.01	91/19	<0.01	35/19	0.01	26/19	0.14

JHEP06(2022)063

Differential cross-sections using "all jets" @ 13 TeV

Particle level
Fiducial

Observable	PWG+Py8 NNPDF30 A14 χ^2/NDF	PWG+Py8 NNPDF30 A14 p-value	MG5_aMC@NLO+Py8 NNPDF30 UE-EE-5 χ^2/NDF	MG5_aMC@NLO+Py8 NNPDF30 UE-EE-5 p-value	PWG+H7.1.3 NNPDF30 A14 χ^2/NDF	PWG+H7.1.3 NNPDF30 A14 p-value	PWG+Py8 (more IFSR) NNPDF30 A14 χ^2/NDF	PWG+Py8 (more IFSR) NNPDF30 A14 p-value	PWG+Py8 (less IFSR) NNPDF30 A14 χ^2/NDF	PWG+Py8 (less IFSR) NNPDF30 A14 p-value
p_{T}^{t}	3.9/9	0.92	3.1/9	0.96	6.2/9	0.72	1.2/9	1.00	7.7/9	0.57
$\lvert y^{t}\rvert$	6.8/10	0.75	5.8/10	0.83	6.8/10	0.74	7.5/10	0.68	5.9/10	0.83
$p_{\mathrm{T}}^{t,1}$	5.1/8	0.75	3.9/8	0.86	5.3/8	0.72	4.3/8	0.83	5.3/8	0.72
$\lvert y^{t,1}\rvert$	6.1/10	0.81	4.7/10	0.91	6.7/10	0.76	5.7/10	0.84	5.6/10	0.84
$p_{\mathrm{T}}^{t,2}$	9.9/8	0.27	10.2/8	0.25	13.9/8	0.08	4.4/8	0.82	16.0/8	0.04
$\lvert y^{t,2}\rvert$	9.4/10	0.49	9.0/10	0.53	9.4/10	0.50	8.9/10	0.54	9.3/10	0.50
$m^{t\bar{t}}$	8.1/12	0.78	6.9/12	0.87	7.4/12	0.83	8.9/12	0.71	7.9/12	0.79
$p_{\mathrm{T}}^{t\bar{t}}$	14.3/8	0.07	35.2/8	< 0.01	24.5/8	< 0.01	2.7/8	0.95	33.5/8	< 0.01
$\lvert y^{t\bar{t}}\rvert$	16.7/10	0.08	17.3/10	0.07	18.1/10	0.05	14.8/10	0.14	17.9/10	0.06
$\chi^{t\bar{t}}$	8.0/11	0.71	10.0/11	0.53	8.1/11	0.71	9.5/11	0.57	12.4/11	0.34
$\lvert y_{\mathrm{B}}^{t\bar{t}}\rvert$	15.3/10	0.12	15.7/10	0.11	16.6/10	0.08	14.1/10	0.17	16.6/10	0.08
$\lvert p_{\mathrm{out}}^{t\bar{t}}\rvert$	17.1/10	0.07	53.6/10	< 0.01	30.9/10	< 0.01	8.6/10	0.57	32.7/10	< 0.01
$H_{\mathrm{T}}^{t\bar{t}}$	5.4/9	0.80	5.0/9	0.83	6.4/9	0.70	3.6/9	0.94	6.8/9	0.66
$\lvert\Delta\phi(t_1,t_2)\rvert$	12.2/7	0.09	73.4/7	< 0.01	23.6/7	< 0.01	5.3/7	0.63	28.5/7	< 0.01
$\lvert\cos\theta^{\star}\rvert$	7.0/10	0.72	9.8/10	0.46	6.8/10	0.74	7.4/10	0.69	10.5/10	0.39
$p_{\mathrm{T}}^{t,1}\otimes p_{\mathrm{T}}^{t,2}$	27.1/15	0.03	27.0/15	0.03	36.7/15	< 0.01	12.0/15	0.68	41.0/15	< 0.01
$\lvert y^{t,1}\rvert\otimes\lvert y^{t,2}\rvert$	11.6/19	0.90	9.8/19	0.96	12.0/19	0.88	14.3/19	0.77	9.7/19	0.96
$\lvert y^{t,1}\rvert\otimes p_{\mathrm{T}}^{t,1}$	8.5/15	0.90	7.6/15	0.94	9.4/15	0.85	9.5/15	0.85	8.4/15	0.91
$\lvert y^{t,2}\rvert\otimes p_{\mathrm{T}}^{t,2}$	15.9/20	0.72	17.1/20	0.65	19.5/20	0.49	10.8/20	0.95	20.7/20	0.41
$p_{\mathrm{T}}^{t,1}\otimes p_{\mathrm{T}}^{t\bar{t}}$	16.1/15	0.37	12.6/15	0.63	26.7/15	0.03	7.3/15	0.95	30.7/15	< 0.01
$p_{\mathrm{T}}^{t,1}\otimes m^{t\bar{t}}$	23.1/18	0.19	21.9/18	0.24	26.7/18	0.08	13.8/18	0.74	30.5/18	0.03
$\lvert y^{t\bar{t}}\rvert\otimes p_{\mathrm{T}}^{t,1}$	14.4/15	0.50	14.5/15	0.49	15.0/15	0.45	12.8/15	0.62	15.6/15	0.41
$\lvert y^{t\bar{t}}\rvert\otimes\lvert y^{t,1}\rvert$	14.7/15	0.47	18.0/15	0.26	15.6/15	0.41	11.6/15	0.71	19.1/15	0.21
$\lvert y^{t,1}\rvert\otimes m^{t\bar{t}}$	20.0/19	0.40	20.1/19	0.39	20.0/19	0.39	19.5/19	0.42	20.3/19	0.38
$\lvert y^{t\bar{t}}\rvert\otimes m^{t\bar{t}}$	12.5/18	0.82	12.1/18	0.84	13.2/18	0.78	12.5/18	0.82	12.9/18	0.80
$p_{\mathrm{T}}^{t\bar{t}}\otimes m^{t\bar{t}}$	20.2/18	0.32	17.9/18	0.46	30.9/18	0.03	9.4/18	0.95	35.2/18	< 0.01
$\lvert y^{t\bar{t}}\rvert\otimes p_{\mathrm{T}}^{t\bar{t}}$	19.1/15	0.21	14.5/15	0.49	29.4/15	0.01	12.2/15	0.66	33.4/15	< 0.01
$\lvert y^{t\bar{t}}\rvert\otimes m^{t\bar{t}}\otimes p_{\mathrm{T}}^{t,1}$	21.9/31	0.88	24.1/31	0.81	24.6/31	0.79	18.0/31	0.97	26.9/31	0.68

arXiv:2205.02817

Differential cross-sections using ”all jets” @ 13 TeV

arXiv:2205.02817

Parton level

Observable	PWG+Py8 NNPDF30 A14		MG5_aMC@NLO+Py8 NNPDF30 UE-EE-5		PWG+H7.1.3 NNPDF30 A14		PWG+Py8 (more IFSR) NNPDF30 A14		PWG+Py8 (less IFSR) NNPDF30 A14	
	χ^2/NDF	p-value	χ^2/NDF	p-value	χ^2/NDF	p-value	χ^2/NDF	p-value	χ^2/NDF	p-value
p_{T}^{t}	3.1/9	0.96	3.7/9	0.93	4.3/9	0.89	1.4/9	1.00	6.2/9	0.72
$\|y^{t}\|$	6.2/10	0.80	6.1/10	0.81	6.0/10	0.82	6.1/10	0.80	5.8/10	0.83
$p_{\mathrm{T}}^{t,1}$	3.2/8	0.92	2.6/8	0.96	3.6/8	0.89	4.0/8	0.86	3.1/8	0.93
$\|y^{t,1}\|$	5.7/10	0.84	5.0/10	0.89	5.9/10	0.82	5.5/10	0.86	5.5/10	0.86
$p_{\mathrm{T}}^{t,2}$	5.4/8	0.71	9.6/8	0.30	5.9/8	0.66	3.2/8	0.92	8.3/8	0.41
$\|y^{t,2}\|$	9.3/10	0.51	9.6/10	0.48	9.2/10	0.51	9.1/10	0.52	9.2/10	0.52
$m^{t\bar{t}}$	7.4/12	0.83	8.6/12	0.73	7.4/12	0.83	7.6/12	0.81	7.1/12	0.85
$p_{\mathrm{T}}^{t\bar{t}}$	7.2/8	0.51	23.5/8	< 0.01	8.6/8	0.38	3.1/8	0.93	13.0/8	0.11
$\|y^{t\bar{t}}\|$	13.1/10	0.22	13.5/10	0.20	13.6/10	0.19	12.1/10	0.28	13.9/10	0.18
$\chi^{t\bar{t}}$	7.6/11	0.74	8.0/11	0.71	8.3/11	0.69	7.4/11	0.77	9.9/11	0.54
$\|y_{\mathrm{B}}^{t\bar{t}}\|$	11.7/10	0.31	12.0/10	0.29	11.7/10	0.31	11.1/10	0.35	12.5/10	0.26
$\|p_{\mathrm{out}}^{t\bar{t}}\|$	7.1/10	0.72	44.9/10	< 0.01	12.5/10	0.25	4.6/10	0.92	11.2/10	0.34
$H_{\mathrm{T}}^{t\bar{t}}$	3.4/9	0.95	3.3/9	0.95	3.8/9	0.93	3.3/9	0.95	3.7/9	0.93
$\|\Delta\phi(t_1,t_2)\|$	10.5/7	0.16	81.1/7	< 0.01	25.9/7	< 0.01	4.2/7	0.76	19.2/7	< 0.01
$\|\cos\theta^{\star}\|$	7.1/10	0.72	7.8/10	0.65	7.5/10	0.67	6.6/10	0.76	8.6/10	0.57
$p_{\mathrm{T}}^{t,1} \otimes p_{\mathrm{T}}^{t,2}$	13.7/15	0.55	23.2/15	0.08	16.5/15	0.35	5.8/15	0.98	22.5/15	0.10
$\|y^{t,1}\| \otimes \|y^{t,2}\|$	9.8/15	0.83	9.6/15	0.85	9.5/15	0.85	10.3/15	0.80	9.2/15	0.86
$\|y^{t,1}\| \otimes p_{\mathrm{T}}^{t,1}$	8.0/15	0.92	7.5/15	0.94	8.6/15	0.90	8.8/15	0.89	8.1/15	0.92
$\|y^{t,2}\| \otimes p_{\mathrm{T}}^{t,2}$	13.5/20	0.86	15.7/20	0.74	13.5/20	0.86	11.3/20	0.94	16.5/20	0.68
$p_{\mathrm{T}}^{t,1} \otimes p_{\mathrm{T}}^{t\bar{t}}$	11.9/15	0.69	21.5/15	0.12	15.4/15	0.42	6.9/15	0.96	22.2/15	0.10
$p_{\mathrm{T}}^{t,1} \otimes m^{t\bar{t}}$	17.8/18	0.47	19.5/18	0.36	17.6/18	0.48	12.9/18	0.80	23.8/18	0.16
$\|y^{t\bar{t}}\| \otimes p_{\mathrm{T}}^{t,1}$	12.0/15	0.68	11.6/15	0.71	11.4/15	0.72	11.5/15	0.71	12.7/15	0.63
$\|y^{t\bar{t}}\| \otimes \|y^{t,1}\|$	14.2/15	0.51	14.7/15	0.47	14.1/15	0.52	12.2/15	0.67	17.2/15	0.31
$\|y^{t,1}\| \otimes m^{t\bar{t}}$	19.0/19	0.46	18.6/19	0.49	19.3/19	0.44	19.0/19	0.46	19.2/19	0.44
$\|y^{t\bar{t}}\| \otimes m^{t\bar{t}}$	12.3/18	0.83	12.1/18	0.84	12.2/18	0.84	13.6/18	0.75	11.8/18	0.86
$p_{\mathrm{T}}^{t\bar{t}} \otimes m^{t\bar{t}}$	25.9/18	0.10	22.0/18	0.23	32.0/18	0.02	13.8/18	0.74	35.2/18	< 0.01
$\|y^{t\bar{t}}\| \otimes p_{\mathrm{T}}^{t\bar{t}}$	13.5/15	0.56	18.9/15	0.22	15.6/15	0.41	12.7/15	0.63	16.3/15	0.36
$\|y^{t\bar{t}}\| \otimes m^{t\bar{t}} \otimes p_{\mathrm{T}}^{t,1}$	15.5/31	0.99	17.9/31	0.97	15.1/31	0.99	15.5/31	0.99	17.7/31	0.97

Are top quarks too central or too forward in models ?

CMS dilepton

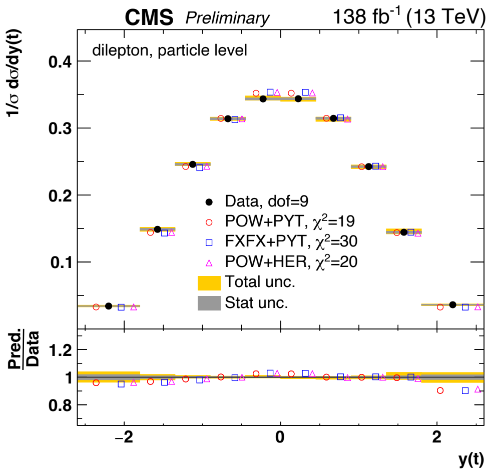

ATLAS dilepton

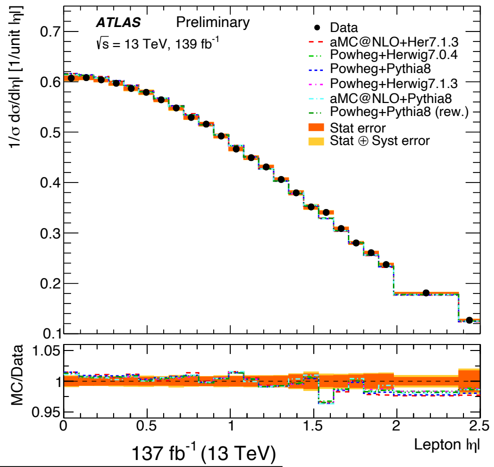

Dileptonic model top quarks look too central

- But not so in other channels

ATLAS l+jet(boosted)

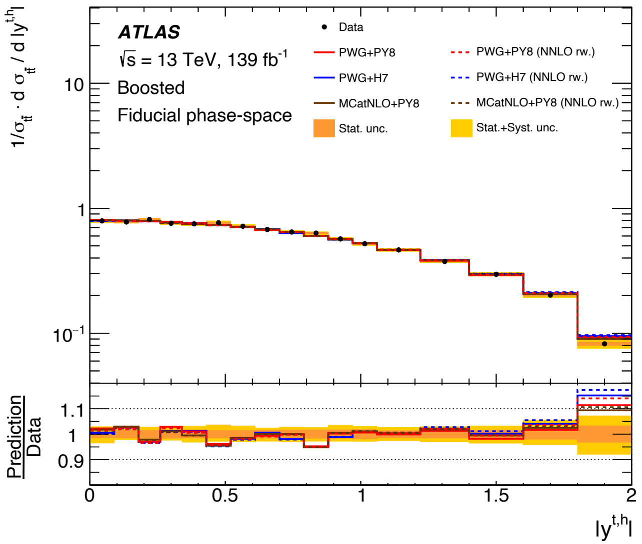

CMS l+jets

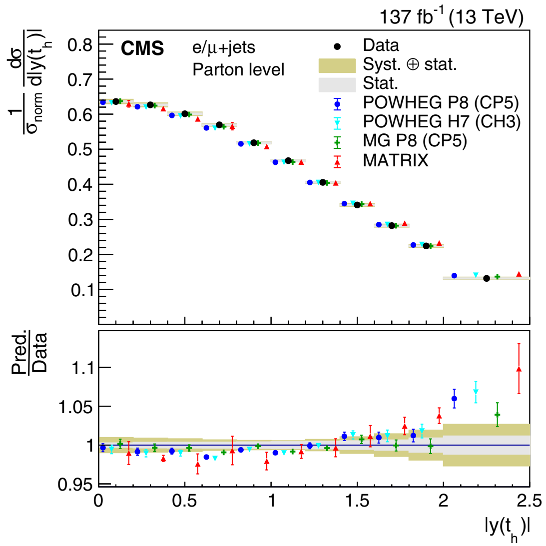

ATLAS all (boosted) jets